Research Square

Preprints are preliminary reports that have not undergone peer review.
They should not be considered conclusive, used to inform clinical practice,
or referenced by the media as validated information.

Gene signature of m6A-related targets to predict prognosis and immunotherapy response in ovarian cancer

Wei Tan (vivitan@whu.edu.cn)
Renmin Hospital of Wuhan University: Wuhan University Renmin Hospital https://orcid.org/0000-0001-8114-8290

Shiyi Liu
Renmin Hospital of Wuhan University: Wuhan University Renmin Hospital

Zhimin Deng
Renmin Hospital of Wuhan University: Wuhan University Renmin Hospital

Fangfang Dai
Renmin Hospital of Wuhan University: Wuhan University Renmin Hospital

Mengqin Yuan
Renmin Hospital of Wuhan University: Wuhan University Renmin Hospital

Wei Hu
Renmin Hospital of Wuhan University: Wuhan University Renmin Hospital

Yanxiang Cheng
Renmin Hospital of Wuhan University: Wuhan University Renmin Hospital

Research Article

Keywords: ovarian cancer, RNA N6-methyladenosine, prognosis, immunotherapy, tumor mutation burden

Posted Date: May 11th, 2022

DOI: https://doi.org/10.21203/rs.3.rs-1556914/v2

License: This work is licensed under a Creative Commons Attribution 4.0 International License.
Read Full License

Abstract

Purpose: The aim of the study was to construct a risk score model based on m6A-related targets to predict overall survival and immunotherapy response in ovarian cancer.

Methods: The gene expression profiles of 24 m6A regulators were extracted. Survival analysis screened 9 prognostic m6A regulators. Next, consensus clustering analysis was applied to identify clusters of ovarian cancer patients. Furthermore, 47 phenotype-related differentially expressed genes, strongly correlated with 9 prognostic m6A regulators, were screened and subjected to univariate and the least absolute shrinkage and selection operator (LASSO) cox regression. Ultimately, a nomogram was constructed which presented a strong ability to predict overall survival in ovarian cancer.

Results: *CBLL1*, *FTO*, *HNRNPC*, *METTL3*, *METTL14*, *WTAP*, *ZC3H13*, *RBM15B* and *YTHDC2* were associated with worse overall survival (OS) in ovarian cancer. Three m6A clusters were identified, which were highly consistent with the three immune phenotypes. What's more, a risk model based on seven m6A-related targets was constructed with distinct prognosis. And the low-risk group are the best candidate population for immunotherapy.

Conclusions: We comprehensively analyzed the m6A modification landscape of ovarian cancer and detected seven m6A-related targets as an independent prognostic biomarker for predicting survival. Furthermore, we divided patients into high- and low- risk groups with distinct prognosis and select the optimum population which may benefit from immunotherapy and constructed a nomogram to precisely predict ovarian cancer patients' survival time and visualize the prediction results.

Introduction

N6-methyladenosine (m6A) is the most common modification of eukaryotic mRNA and lncRNA, playing a key role in epigenetics (Xu et al. 2022). The methylation modification of m6A is reversible, and the regulatory factors include methyltransferases (METTL3/14/16, WTAP, RBM15/15B, RBMX, CBLL1, and ZC3H13, termed "writers"), demethylase (FTO and ALKBH5, termed "erasers") and methylated reading protein (YTHDC1/2, YTHDF1/2/3, IGF2BP1/2/3, HNRNPC, LRPPRC, HNRNPA2B1, and EIF3, termed "readers") (Chen et al. 2020, Fan et al. 2020). M6A regulators affect the processing, transportation, and translation of mRNA, activation of immune responses, and cell fate decisions (Chen et al. 2020, Shulman and Stern-Ginossar 2020). Sufficient evidence suggested that aberrant expression and genetic alteration of m6A regulators were closely related to pathogenesis of cancers (Yue et al. 2019, Zhang et al. 2020). Ovarian cancer is the fifth leading cause of mortality among adult women, according to cancer statistics for 2021 (Siegel et al. 2021). Until now, METTL3, ALKBH5, FTO, YTHDF1 and YTHDF2 had been proved that participated in the process of proliferation and migration of ovarian cancer (Li et al. 2020, Xu et al. 2021, Hao et al. 2021, Bi et al. 2021, Jiang et al. 2020).

Generally, different m6A regulators might have distinct functions. However, even the identical m6A regulators may have distinct functions under distinct conditions, mainly due to distinct downstream

targeted genes. Liu et al. reported that METTL3 could interact with CUL4B, and then active PI3K/AKT signaling pathway, which plays a pivotal role in promoting gastric cancer progression (Liu et al. 2021). Xia et al. discovered that METTL3 is involved in apoptosis mediated by Keap1/Nrf2 signaling pathway (Xia et al. 2021). Therefore, identification of the targets of m6A regulators is particularly important to elucidate the dynamic variation.

Sequencing technology has developed tremendously over the past decades, and subsequently genetic and epigenetic therapies began to emerge. So far, there are two gene-related therapeutic strategies, namely targeted and immunotherapy. Disappointingly, for the unscreened population, most patients benefit little or nothing from immunotherapy, far from meeting clinical needs (Zhang et al. 2020). In general, immunotherapy is closely related to the tumor microenvironment (TME), such as T cell abundance and tumor mutation burden (TMB) (Zhang et al. 2020, Galon and Bruni 2019). M6A also played a crucial role in TME (Xia et al. 2021). In this paper, our bold conjecture is that m6A can influence the efficacy of immunotherapy by acting on downstream targets and TME.

In the current work, we screened 9 prognostic m6A regulators, and identified three modification patterns. Next, we identified 7 m6A-related mRNAs and disclosed that they may be potential target of m6A regulators using the m6A2Target database. We also constructed a risk score model to predict overall survival and immunotherapy response. Overall, the low-risk group was more suitable for immunotherapy. Finally, seven identified m6A-related targets were validated with quantitative PCR and the Human Protein Atlas (HPA) database. The flow of the study was shown in Fig. 1.

Materials And Methods

Data collection and preprocessing

The expression profiles and clinical information of ovarian cancer were obtained from The Cancer Genome Atlas (TCGA, https://portal.gdc.cancer.gov/) and GSE140082 (GPL14951). On the other hand, the expression matrix of normal ovarian tissue was acquired from the Genotype-Tissue Expression (GTEx, http://commonfund.nih.gov/GTEx/data). Next, we used “ComBat” function of sva package to correct non-biological batch effects. The somatic mutation data and Copy Number Variation (CNV) were obtained from TCGA dataset. Then, the correlation between m6A expression and CNV patterns was analyzed using the Kruskal-Wallis tests. In addition, the ‘oncoplot’ function of R package ‘maftools’ was utilized to depict the mutation landscape. The RCircos package in R software was chosen to visualize the m6A regulators in chromosomes (Mayakonda et al. 2018).

Unsupervised clustering for 9 m6A regulators and differential expression analysis

We selected 24 m6A methylation regulators from the previous publications for this study (Fan et al. 2020, Wang et al. 2021). Kaplan–Meier (KM) survival analysis was chosen to compare the OS of ovarian cancer patients in distinct m6A groups. And 9 m6A regulators were screened. Unsupervised clustering

analysis was performed to identify different m6A clusters based on 9 prognostic m6A regulators. The R package “ConsensuClusterPlus” was adopted to perform the steps (Wilkerson and Hayes 2010).

Functional annotation between different m6A clusters

Overlapping differentially expressed genes among different m6A clusters were screened using R “limma” package. $P < 0.001$ and |logFC| > 0.5 were set as the inclusion criteria. The Search Tool for the Retrieval of Interacting Genes (STRING, https://cn.string-db.org/) protein database and cytoscape was utilized to construct the Protein-protein interactions (PPI) and co-expression networks (Szklarczyk et al. 2015). GSVA algorithm was performed using the R “GSVA” package (Hanzelmann et al. 2013). Finally, based on overlapped differentially expressed genes (DEGs), Gene Ontology (GO) and Kyoto Encyclopedia of Genes and Genomes (KEGG) enrichment analyses were conducted. The significance criteria were set as an adjusted $p < 0.05$ and |logFC | > 0.1.

Estimation of immune cell infiltration

The single sample gene set enrichment analysis (ssGSEA) algorithm was employed to quantify the level of immune cell infiltration(Subramanian et al. 2005, Barbie et al. 2009). The gene set that labeled each immune cell type was derived from Charoentong's study (Charoentong et al. 2017). Immunophenotypic scores (IPS) of ovarian cancer patients were obtained from The Cancer Immunome (TCIA, https://tcia.at/home) database, which can reflect the efficacy of immune checkpoint blockade (ICB) immunotherapy (Charoentong et al. 2017).

Construction of the risk score model

Univariate Cox regression analysis was applied to screen prognostic genes using R “Survival” package. $P < 0.05$ was set as the inclusion criteria. 98 prognostic genes were screened. Next, ‘pacman’ package in R software was applied to conduct ‘pearson’ correlation analysis. The inclusion criteria were set as $p < 0.05$ and |cor| > 0.3. Finally, the least absolute shrinkage and selection operator (LASSO) regression was employed to further screen for potential prognostic risk characteristics.

$$\text{Risk Score} = 0.063 * ELK3 + 0.024 * AFF4 + 0.016 * RCOR2 + 0.014 * PHATCR2 + 0.013 * CIZ1 + 0.061 * NUAK1 + 0.070 * MCC$$

The R “Survminer” package was utilized to determine cutoff points, and then divided the patients into the high- and low-risk group according to cutoff points. The transcriptional profiles were compared by principal component analysis (PCA) and t-distributed stochastic neighbor embedding (t-SNE).

Establishment and validation of a prognostic nomogram

The prognostic value of the risk score was accessed by the univariate and multivariable Cox regression analyses. The R packages “forestplot” were employed to visualize the results. The clinical information,

including age, stage and grade were adopted for model correction. Next, a nomogram was established by multivariate Cox regression. Then, the calibration plots and the C-index were calculated for the nomogram models. These analyses were executed by the R package “rms.” Receiver operating characteristic (ROC) (R package “survivalROC”) curves were constructed to evaluate the prognostic ability of the nomogram for 1/3/5-year OS and the area under the curve (AUC) values.

Validation of the expression of the genes in risk signature

All the specimens were from the Gynecology in Renmin Hospital of Wuhan University. All the patients provided informed consent and were approved by the Ethics Committee of Renmin Hospital of Wuhan University. We collected contralateral normal ovarian tissue from 3 cases with ovarian cysts and ovarian cancer tissue of 5 cases. Total RNA was isolated with TRIzon reagent (Invitrogen). Primers used in the qRT-PCR are present in Supplementary file 8. Reverse transcription was performed using mRNA Reverse-Transcription Kit (Yeasen Biotech Co., Ltd.) according to the manufacturer’s instruction. Random primers were added to initiate cDNA synthesis. qRT-PCR was executed using the SYBR Green PCR Mix (Yeasen Biotech Co., Ltd.) on a Bio-Rad CFX96 system. The $2^{-\Delta\Delta Ct}$ method was performed to calculate the gene relative expression. In addition, to further determine the expression level of the m6A-related genes, immunohistochemical images were obtained from the HPA database (https://www.proteinatlas.org/).

Potential targets of m6A regulators

The validated and potential targets of m6A regulators were obtained from the m6A2Target databases (Deng et al. 2021).

Statistics

When the samples are divided into two groups, if the samples meet the parameter conditions (normal distribution and homogeneity of variance), t test is employed, otherwise the non-parametric two-sided Wilcoxon-rank sum test was chosen. Furthermore, when the samples were divided into multiple groups, ANOVA test was performed if the samples met parameter conditions, otherwise Kruskal-Wallis tests was employed. The R package “limma” was employed to identify differential transcription factors in distinct group (Ritchie et al. 2015). The threshold for differential transcription factor were as follows: $p < 0.05$(“*”), $p < 0.01$(“**”), $p < 0.001$(“***”). $P < 0.05$ was regarded as significant. All analyses were performed with R software V4.1.0 and GraphPad Prism.

Results

Genetic alteration of m6A regulators in ovarian cancer

In TCGA cohort, nine out of 21 m6A regulators (RBM15, RBM15B, LRPPRC, ZC3H13, IGF2BP2, CBLL1, YTHDF1/2/3, and ELAVL1) had significantly high expression level in ovarian cancer. While the expression of METTL3/14/16, WTAP, FTO, HNRNPA2B1, HNRNPC, YTHDC1/2 and RBMXwere decreased in ovarian

cancer (Fig. S1A, S1C). Furthermore, K-M analysis was carried out to evaluate the clinical significance of the 24 m6A regulators in ovarian cancer, nine of them were correlated with the overall survival (OS) (Fig. 2). The patients with over-expressions of METTL3, HNRNPC and YTHDC2 had longer OS. The PPI analysis revealed that WTAP, RBM15, METTL3, METTL14, FTO and HNRNPA2B1 had more internal connections with others, while *I*GF2BP2, IGF2BP1, IGF2BP3, LRPPRC and EIF3A had less interaction with others (Fig. S2A). In addition, except for IGF2BP1, there were significant positive correlations between m6A regulatory factors (Fig. S2B).

The somatic mutations of 24 m6A regulators were mapped in Figure S1B, which showed that the mutations in m6A regulators were rarely observed in ovarian cancer. Only 11.7% of the 436 patients had somatic mutations, and m6A “reader” YTHDF1had the highest frequency of mutations in ovarian cancer (Fig. S1B, Supplementary file 8). By the contrast, a larger number of broad CNVs were existed in m6A regulators, and most of which leads to amplification, but deletion of YTHDF2, YTHDC2, RBM15B and WTAP (Fig. S1D, Supplementary file 8). Furthermore, CNV has been proved that positively correlated with the expression of m6A regulators (Fig. S3). In summary, CNVs may contribute to the abnormal expression of m6A regulators, and further effected the progression and clinical outcomes of ovarian cancer.

Consensus clustering of m6A regulators in ovarian cancer

Figure 3A showed the crosslink among the 24 m6A regulators and their clinical significance (Fig. 3A). We observed the significant crosslink not only existed in the m6A regulators with same function, but also between the “writers”, “erasers” and “readers”. The above results suggested that the interconnection of the “writers”, “erasers” and “readers” might form a variety of modification patterns in ovarian cancer. The cohort was divided into three subgroups (m6Acluster A: N = 266; m6Acluster B: N = 183; m6Acluster C: N = 307) by applying the unsupervised clustering of nine prognostic m6A regulators. The optimal number of stable gene clusters were three (k = 3) by the consistent clustering algorithm (Fig. S2C). A clear separation was observed among them (Fig. S2D). Next, we compared OS between each cluster and proved that m6Acluster B had decreased OS than m6Acluster A and m6Acluster C (p = 0.015, Fig. 3B). Nevertheless, there was no statistical difference in OS between m6Acluster A and m6Acluster C. Notably, ovarian cancer patients in m6Acluster B had more expression of m6A (Fig. 3C).

As shown in the Fig. S4, metabolic pathways like inositol phosphate, glutathione metabolism and oxidative phosphorylation were enriched in m6Acluster A. While m6Acluster B were significantly related to carcinogenesis, including TGF-β signaling, Notch signaling, Hedgehog signaling, WNT signaling and ubiquitin mediated proteolysis (Fig. S4A-B) (Batlle and Massague 2019, Meurette and Mehlen 2018, Doheny et al. 2020, Katoh and Katoh 2020, Jiang et al. 2020). The above results suggested that m6A regulators were involved in many crucial cellular activities, such as carcinogenesis, and inflammation of ovarian cancer.

Immune landscape was significantly associated with the m6A modification pattern

Infiltration of immune cells within the TME have a pivotal role on the tumor progression and the efficacy of immunotherapy. The infiltration of B cells, $CD4^+$ T cells, $CD8^+$ T cells, dendritic cells, NK cells and T helper cell was low in m6A cluster B which presented immune-excluded patterns (Fig. 4A). Additionally, we explored associations between 9 prognostic factors and 23 types of immune cells and found that most of the m6A were negatively correlated with immune cells, except for METTL14 and WTAP (Fig. 4B).

Construction and verification of the m6A-score model

357 overlapping differentially expressed genes among the m6Acluster A, m6Acluster B and m6Acluster C were identified in this study ($p < 0.001$, $|logFC| > 0.5$, Fig. S5A). The result of GO analyses showed that overlapping differentially expressional genes (DEGs) were related to cell surface receptor, protein kinase activity, extracellular matrix, and cytoplasmic region (Fig. S5C). In the tumor-associated signaling pathway, KEGG analysis suggested that overlapping DEGs were enriched in PI3K-Akt signing pathway, focal adhesion, and ECM-receptor interaction (Supplementary file 8).

Then, 97 overlapping DEGs were correlated with prognosis by univariate cox analysis ($p < 0.05$) (Supplementary file 8). The correlation between 97 genes and 9 prognostic m6A regulators was analyzed, and shown in Figure S5B. As shown in Fig. 5B, 47 genes were strongly correlated with 9 prognostic m6A regulators ($p < 0.05$, $|cor| > 0.3$). Furthermore, co-expression network of the m6A-related genes and m6A regulators was plotted (Fig. S5D).

To avoid over-fitting of the prognostic model, 47 differentially expressed m6A-related genes with prognostic values were analyzed by LASSO regression analysis, and 7 genes were screened for prognostic model (Fig. 5A-B). With the cutoff value 6.018, patients were divided into high or low-risk groups (Supplementary file 8). Encouragingly, the results from m6A2Target database demonstrated that the seven genes are potential targets for 9 m6A regulators (Supplementary file 8) (Cheng et al. 2019). There was a better prognosis in low-risk group ($p < 0.001$, Fig. 5C). The area under ROC curve was 0.627 (Fig. 5D). Moreover, PCA and t-SNE showed that the two groups were presented in two different patterns (Fig. 5E-F).

We likewise examined the correlation between risk score and clinical characteristics. There was differential expression of risk scores between different grades. The risk score of G1-2 is higher than that of G3-4 (Fig. S6A). Due to the difficulty in early detection of ovarian cancer, most clinical samples were found to be in the middle and advanced stages, so the number of patients with G1-2 was slight, and the experimental results may be biased. Although the box plot showed risk scores at an advanced stage as well as age > 65 had higher levels, but this was not statistically significant (Fig. S6B-C). Additionally, we respectively studied the influence of risk group on prognosis under different clinical characteristics, and the results proved that, in all clinical subgroups, the prognosis was better in low-risk group (Fig. S6D-F). In the prognostic model, the risk scores and the number of deaths were elevated in high-risk group (Fig. S6G).

Evaluation of the correlation between prognostic risk score and ICBs

Immunotherapy represented by ICBs has shown impressive therapeutic efficacy with long-lasting responses in a minor subset of patients. In general, immunotherapy is closely related to TME, like T cell abundance and TMB. Thus, we compared the scores related to TME between two groups and hoped to screen the optimal groups for immunotherapy.

The stromal score was significantly elevated in high-risk group (Fig. 6A). However, there was no significant difference in the immune score. We next investigated the immune infiltration in two groups. The resulted indicated that patients in high-risk group had enhanced adaptive infiltrating immune cells, including eosinophil, macrophages, mast cell, dendritic cell, and regulatory T cell et al. On the other hand, activated B cell, $CD4^+$ and $CD8^+$ T cell, and type 17 helper cell had been discovered to be mostly enriched in low-risk group (Fig. 6B). The above results showed that it was the proportion of immune cells, rather than the content of immune cells, that differed between the two groups. Furthermore, the results of immune-related pathways elucidated that cytolytic activity, HLA, inflammation promoting, T cell co-stimulation and type I interferon (IFN) response were significantly elevated in low-risk group. High-risk group had a higher enrichment of type II IFN response, which plays critical roles in orchestrating both innate and adaptive immune responses (Fig. 6C). Next, we compared the expression of 9 prognostic m6A regulators between two groups. The results demonstrated that the high-risk group had higher expression of m6A regulators (Fig. 6E). Ultimately, the tumor biology-related signaling pathways were analyzed and the results indicated that cell proliferation, DNA repair, and EMT related signaling pathways were enriched in high-risk group (Fig. 6D-G).

The discovery of immune checkpoints and the development of immune checkpoint inhibitors have opened a new chapter in the war on cancer. Immune checkpoints CD80, CD276, CD86, LGALS9, PDCD1LG2, CD44, LAIR1, TNFSF4, NRP1, TNFSF9, CD28, HAVCR2, CD200were significantly upregulated in high-risk score, showing a consistent trend with poor prognosis (Fig. 7A). In addition, IPS was higher in low-risk group, implicating a better response to ICBs therapy (Fig. 7B).

TMB was regard as a specific marker to guide the ICBs. Higher TMB was higher neo-antigenicity, which subsequently improved the response of ICBs in tumors. The R package “maftools” was performed to analyze the effect of TMB on the survival prognosis of ovarian cancer, our results revealed that the higher TMB was correlated with better prognosis (Fig. 7D). TMB was integrated with risk score for prognosis analysis, and the results demonstrated that patients in the group with low risk-score and high TMB had the best survival prognosis compared with the other three groups (Fig. 7E). Subsequently, we investigated the association between TMB and risk-score and compared the differences in the distribution of somatic mutations between high- and low-risk groups and observed a negative correlation between TMB and risk score, and the TMB was higher in the low-risk group, but there was no statistic difference (Fig. 7C). In short, the burden of tumor mutations was more extensive in the low-risk group (95.88 vs. 94.17%) (Fig. 7G-H). The correlation between risk score and TMB is not significant, which may be related to insufficient samples.

Validation of the m6A signature

We referred risk score as independent protective factor ($p < 0.001$, 95% CI HR: 1.215-1.516) (Fig. 8A), and this association remained statistically significant ($p < 0.001$, 95%CI HR: 1.195-1.486) after adjusting for age, stage, and grade (Fig. 8B).

To provide a quantitative method to predict the probability of survival, we constructed a nomogram that integrated both the risk score and clinical characteristics (Fig. 8D). The calibration plots depicted in Figure 8E showed that the derived nomogram performed well. Similarly, nomogram model showed predictive ability at 1, 3 and 5-year overall survivals (1-year AUC = 0.679, 3-year AUC = 0.661, 5-year AUC = 0.624) (Fig. 8F). Integration of the risk score with clinical characteristics in the nomogram showed high specificity and sensitivity of survival prediction. To further confirm the expression of the seven prognostic genes, we obtained ovarian cancer and normal ovary tissues from patients including 5 cancer samples and 3 normal tissues. The results demonstrated that almost genes were significantly downregulated in ovarian cancer (Fig. 8C). Additionally, the representative immunohistochemical images from the HPA database were obtained. And the results were in line with qRT-PCR (Figure S7).

Discussion

Ovarian cancer is a heterogeneous disease. Even among patients with similar characteristics and clinical stage, the prognosis may vary greatly. Accumulated evidence showed that m6A modification by targeting downstream genes played a considerable role in tumor proliferation, differentiation, development, invasion, and metastasis (Xu et al. 2021, Hua et al. 2018, Liu et al. 2020, Liu et al. 2018). Accumulated evidence reveled that m6A regulators and their targets may play a crucial role in the benefit of immunotherapy (Cong et al. 2021, Song et al. 2021, Liu et al. 2021). Yet, the studies to date have tended to focus on m6A regulators rather than their targets and far too little attention has been paid to the potential role of m6A regulators and their targets influencing ovarian cancer immunotherapy. Hence, this study was undertaken to investigate the potential functions of m6A regulators and their targets and identify the candidate crowd that would benefit from ICB therapy.

In this work, we compared the different expressions of normal tissues with 24 m6A regulators of ovarian cancer patients, and then screened out 9 prognostic m6A which revealed three m6A modification patterns with different TME cell infiltration in the landscape, which were highly consistent with the three immune phenotypes, including immune rejection, immune inflammation, and immune desert (Zhang et al. 2020). What's more, we researched the mutation of m6A and CNV in ovarian cancer. The results indicated that CNV rather than mutation was closely related to m6A expression. Significantly, compared to the other two groups, m6Acluster B had the worst prognosis, with an infiltrative feature of immunosuppression. Additionally, the result of GSVA demonstrated that malignant functional features of the tumor were significantly enriched in m6Acluster B. Considering the heterogeneity of m6A modification, we selected 97 overlapping DEGs which were correlated with prognosis of three m6A clusters to quantify the pattern of m6A modification in individual tumors. The signature genes and signal pathway in current work can provide ideas for laboratory experimental design to elucidate the molecular mechanism of ovarian cancer. Next, results from LASSO analysis revealed seven key genes, namely, ELK3, AFF4, RCOR2,

PHACTR2, CIZ1, NUAK1, and MCC. ELK3 plays a key role in the migration and apoptosis of cancers and is associated with infiltration of M2 macrophages, $CD4^+$ and $CD8^+$ T cell (Yang et al. 2020, Dazhi et al. 2020, Meng et al. 2020, Kim et al. 2020). AFF4 is a validated downstream target of m6A regulators and participates the migration and growth of tumor (Wu et al. 2021, Liang et al. 2018). Cheng disclosed that METTL3 could promote the bladder cancer progression via AFF4/NF-κB/MYC signaling network (Cheng et al. 2019). RCOR2 is known as an immunomodulatory gene and is related with $CD8^+$ T cell (Routh et al. 2020). Park and colleges demonstrated that RCOR2, RCOR1, RCOR3 form a core ternary transcriptional repressor complex LSD1, which regulating transformation and tumorigenesis (Park et al. 2020). Xiong (Xiong et al. 2020) proved that RCOR1, RCOR2, and LSD1 impaired Foxp3 + Treg function and promoted antitumor immunity. PHACTR2 is identified as a candidate gene for lung cancer and can contribute to the DNA repair capacity (Musolf et al. 2021, Wang et al. 2013). CIZ1 is a driver of tumorigenesis by regulating cell cycle and apoptosis (Chen et al. 2019, Pauzaite et al. 2016). Higgins elucidated that CIZ1 is a circulating biomarker for lung cancer (Higgins et al. 2012). NUAK1, a member of ARK5 family, is implicated in inhibiting tumor cell apoptosis and tumor cell invasion and metastasis (Monteverde et al. 2018). There is an abundance of evidence that the expression of NUAK1 is negatively correlated with prognosis in ovarian cancer (Phippen et al. 2016, Zhang et al. 2015, Riester et al. 2014). MCC is a tumor suppressor in colorectal cancer (Kinzler et al. 1991). Abundant studies reported that the expression of MCC is decreased in many cancers, and re-expression of MCC could inhibit cell proliferation (Fukuyama et al. 2008, Xiao et al. 2017).

To further explore the prognostic value and biological mechanisms of key targets, we constructed a m6A-related prognostic model to provide novel insights for the treatment of ovarian cancer. According to the best cutoff value of the risk score, the patients were stratified into high- and low-risk subgroups with different clinical outcomes. Moreover, the results of PCA and t-SNE showed that the risk model is discriminative. Next, we investigated the relationship between the risk score and clinical features and discovered that it was strongly associated with prognosis.

The tumor microenvironment continually changes over the course of cancer progression and the composition of the tumor microenvironment influences the response of the ICB. Usually, the responses to ICB therapy depends on the TMB and tumor-infiltrating lymphocytes (Li et al. 2020). To explore whether there is a possible connection between ICB therapy and risk score, we researched the immune-infiltrating and TMB in high- and low-risk groups. There was no statistically significant difference in immune scores. In addition, patients in high-risk groups had enhanced adaptive infiltrating immune cells, including eosinophil, macrophages, mast cell, dendritic cell, and regulatory T cell et al. On the other hand, activated B cell, activated $CD4^+$ and $CD8^+$ T cell, and type 17 helper cell had been discovered to be mostly enriched in low-risk group. The findings indicated that the difference between the two groups is the proportion of immune cells rather than the total amount of immune cells. Moreover, cytolytic activity, HLA, inflammation promoting, T cell co-stimulation and type I IFN response were significantly elevated in low-risk group. High-risk group had a higher enrichment of type II IFN response, which plays critical roles in orchestrating both innate and adaptive immune responses (Lazear et al. 2019). These results indicated

that adaptive immune responses were weaker in high-risk group, which may be associated with poor prognosis. Ultimately, we discovered that cell proliferation, DNA repair, and EMT related signaling pathways were enhanced in high-risk group. Additionally, we explored the expressions of several key immune checkpoints and found that the expression levels of IDO1, VTCN1 and LGALS9 in low-risk group were higher. Higher TMB has higher neo-antigenicity, which subsequently improved the response of ICBs in tumors. We combined TMB and risk score to divide the population into four groups for prognostic survival analysis. The results elucidated that there was a best prognosis in high-TMB and low-risk subgroup. Moreover, IPS can effectively predict the effect of tumor immunotherapy. We detected that the IPS of the low-risk group was higher, suggesting that the low-risk group might be the best candidate to receive ICB.

Importantly, we demonstrated that the risk score has a good clinical prognostic stratification effect in advanced ovarian cancer. Univariate and multivariate analyses demonstrated that risk score was an independent prognostic factor for ovarian cancer. What's more, integrating other clinical features, we constructed a nomogram to precisely predict ovarian cancer patients' survival time and visualize the prediction results. Emerging sequencing technologies make it possible to individualize risk stratification and treatment at the molecular level. In this work, we innovatively combined risk score to construct a clinical powerful model for prediction of prognosis and ICBs.

Undeniably, there are several limitations in this study. First, we only use m6A2Target database to verify the m6A targets. Further experimental studies are needed to confirm the regulation of m6A modification on these targets and elucidate its role in ovarian cancer progression and immune escape. Secondly, all data came from public databases, undermining the future applicability of the results to the clinic, and we only determined the cutoff value based on the data of TCGA and GSE140082 to distinguish the two groups of high and low scores. Hence, large sample multi-center prospective are warranted to verify our risk model grouping and judgment of immune clustering effect and enhance clinical applicability, which may be our follow-up experimental plan. Finally, about the threshold of risk grouping, there may be some bias, and the best cutoff value still needs more research to explore and confirm. Even so, the rapid development of biological technologies will hopefully exploit the way for its realization.

Despite these limitations, our study disclosed that the CNVs may contribute to the dysregulation of m6A regulators, and identified three m6A modification patterns with distinct immune landscape. We then identified the overlapped DEGs in three m6A modification patterns and screened m6A-related targets using correlation analysis and m6A2Target database. Overall, we detected seven m6A-related targets as an independent prognostic biomarker for predicting survival. We comprehensively analyzed immune-infiltrating, immune-related pathways, tumor biology-related signaling pathways, immune checkpoints, IPS and TMB between high- and low-risk group and revealed that the low-risk group are the best candidate population for immunotherapy.

In this study, we disclosed that the CNVs may contribute to the dysregulation of m6A regulators, and identified three m6A modification patterns with distinct immune landscape. We then identified the

overlapped DEGs in three m6A modification patterns and screened m6A-related targets using correlation analysis and m6A2Target database. Overall, we detected seven m6A-related targets as an independent prognostic biomarker for predicting survival. Ultimately, we comprehensively analyzed immune-infiltrating, immune-related pathways, tumor biology-related signaling pathways, immune checkpoints, IPS and TMB between high- and low-risk group and revealed that the low-risk group are the best candidate population for immunotherapy.

Declarations

Funding

This work was supported by Key Research and Development Program of Hubei Province (grant number 2020BCB023); the National Natural Science Foundation of China (grant number 82071655, 81860276); Young Teacher Qualification Project of the Fundamental Research Funds for the Central Universities (2042020kf0088); China Medical Association Clinical Medical Research Special Fund Project (grant number 17020310700); the Fundamental Research Funds for the Central Universities (grant number 2042020kf1013); Educational and Teaching Reform Research Project (grant number 413200095) and Graduate credit course projects (grant number 413000206).

Competing interests

The authors have no relevant financial or non-financial interests to disclose.

Authors' Contributions

F-FD and S-YL collected and initially screened the data. WH, F-FD and Y-XC guided the research ideas of the full text. WT performed a visual analysis of the data and was the main contributor to the manuscript. Z-MD improved the writing style and addressed grammatical errors. All authors read and approved the final manuscript.

Data Availability

Publicly available datasets were analyzed in this study. The datasets generated and/or analyzed during the current study are available in the GEO repository (https://www.ncbi.nlm.nih.gov/geo/query/acc.cgi?acc=GSE140082) , TCGA datasets (https://portal.gdc.cancer.gov/legacy-archive/search/f) and **GTEx (**https://commonfund.nih.gov/GTEx/). Additional data not presented in the manuscript can be obtained by contacting the authors.

Ethics approval

This study was approved by Ethics Committee of the Renmin Hospital of Wuhan university, and carried out following the Declaration of Helsinki.

Consent to participate

Informed consent was obtained from all individual participants included in the study.

Consent for publish

Not applicable.

References

1. Xu T, He B, Sun H, Xiong M, Nie J, Wang S et al (2022) Novel insights into the interaction between N6-methyladenosine modification and circular RNA. Mol Ther Nucleic Acids. 27:824-837. 10.1016/j.omtn.2022.01.007
2. Chen Y, Lin Y, Shu Y, He J, Gao W (2020) Interaction between N(6)-methyladenosine (m(6)A) modification and noncoding RNAs in cancer. Mol Cancer. 19(1):94. 10.1186/s12943-020-01207-4
3. Fan L, Lin Y, Lei H, Shu G, He L, Yan Z et al (2020) A newly defined risk signature, consisting of three m(6)A RNA methylation regulators, predicts the prognosis of ovarian cancer. Aging (Albany NY). 12(18):18453-18475. 10.18632/aging.103811
4. Shulman Z, Stern-Ginossar N (2020) The RNA modification N(6)-methyladenosine as a novel regulator of the immune system. Nat Immunol. 21(5):501-512. 10.1038/s41590-020-0650-4
5. Yue B, Song C, Yang L, Cui R, Cheng X, Zhang Z et al (2019) METTL3-mediated N6-methyladenosine modification is critical for epithelial-mesenchymal transition and metastasis of gastric cancer. Mol Cancer. 18(1):142. 10.1186/s12943-019-1065-4
6. Zhang C, Huang S, Zhuang H, Ruan S, Zhou Z, Huang K et al (2020) YTHDF2 promotes the liver cancer stem cell phenotype and cancer metastasis by regulating OCT4 expression via m6A RNA methylation. Oncogene. 39(23):4507-4518. 10.1038/s41388-020-1303-7
7. Siegel RL, Miller KD, Fuchs HE, Jemal A (2021) Cancer Statistics, 2021. CA Cancer J Clin. 71(1):7-33. 10.3322/caac.21654
8. Li J, Wu L, Pei M, Zhang Y (2020) YTHDF2, a protein repressed by miR-145, regulates proliferation, apoptosis, and migration in ovarian cancer cells. J Ovarian Res. 13(1):111. 10.1186/s13048-020-00717-5
9. Xu F, Li J, Ni M, Cheng J, Zhao H, Wang S et al (2021) FBW7 suppresses ovarian cancer development by targeting the N(6)-methyladenosine binding protein YTHDF2. Mol Cancer. 20(1):45. 10.1186/s12943-021-01340-8
10. Hao L, Wang JM, Liu BQ, Yan J, Li C, Jiang JY et al (2021) m6A-YTHDF1-mediated TRIM29 upregulation facilitates the stem cell-like phenotype of cisplatin-resistant ovarian cancer cells. Biochim Biophys Acta Mol Cell Res. 1868(1):118878. 10.1016/j.bbamcr.2020.118878
11. Bi X, Lv X, Liu D, Guo H, Yao G, Wang L et al (2021) METTL3-mediated maturation of miR-126-5p promotes ovarian cancer progression via PTEN-mediated PI3K/Akt/mTOR pathway. Cancer Gene Ther. 28(3-4):335-349. 10.1038/s41417-020-00222-3

12. Jiang Y, Wan Y, Gong M, Zhou S, Qiu J, Cheng W (2020) RNA demethylase ALKBH5 promotes ovarian carcinogenesis in a simulated tumour microenvironment through stimulating NF-kappaB pathway. J Cell Mol Med. 24(11):6137-6148. 10.1111/jcmm.15228
13. Liu HT, Zou YX, Zhu WJ, Sen L, Zhang GH, Ma RR et al (2021) lncRNA THAP7-AS1, transcriptionally activated by SP1 and post-transcriptionally stabilized by METTL3-mediated m6A modification, exerts oncogenic properties by improving CUL4B entry into the nucleus. Cell Death Differ. 10.1038/s41418-021-00879-9
14. Xia C, Wang J, Wu Z, Miao Y, Chen C, Li R et al (2021) METTL3-mediated M6A methylation modification is involved in colistin-induced nephrotoxicity through apoptosis mediated by Keap1/Nrf2 signaling pathway. Toxicology. 462:152961. 10.1016/j.tox.2021.152961
15. Zhang B, Wu Q, Li B, Wang D, Wang L, Zhou YL (2020) m(6)A regulator-mediated methylation modification patterns and tumor microenvironment infiltration characterization in gastric cancer. Mol Cancer. 19(1):53. 10.1186/s12943-020-01170-0
16. Zhang Y, Yang M, Ng DM, Haleem M, Yi T, Hu S et al (2020) Multi-omics Data Analyses Construct TME and Identify the Immune-Related Prognosis Signatures in Human LUAD. Mol Ther Nucleic Acids. 21:860-873. 10.1016/j.omtn.2020.07.024
17. Galon J, Bruni D (2019) Approaches to treat immune hot, altered and cold tumours with combination immunotherapies. Nat Rev Drug Discov. 18(3):197-218. 10.1038/s41573-018-0007-y
18. Mayakonda A, Lin DC, Assenov Y, Plass C, Koeffler HP (2018) Maftools: efficient and comprehensive analysis of somatic variants in cancer. Genome Res. 28(11):1747-1756. 10.1101/gr.239244.118
19. Wang Q, Zhang Q, Li Q, Zhang J, Zhang J (2021) Clinicopathological and immunological characterization of RNA m(6) A methylation regulators in ovarian cancer. Mol Genet Genomic Med. 9(1):e1547. 10.1002/mgg3.1547
20. Wilkerson MD, Hayes DN (2010) ConsensusClusterPlus: a class discovery tool with confidence assessments and item tracking. Bioinformatics. 26(12):1572-1573. 10.1093/bioinformatics/btq170
21. Szklarczyk D, Franceschini A, Wyder S, Forslund K, Heller D, Huerta-Cepas J et al (2015) STRING v10: protein-protein interaction networks, integrated over the tree of life. Nucleic Acids Res. 43(Database issue):D447-452. 10.1093/nar/gku1003
22. Hanzelmann S, Castelo R, Guinney J (2013) GSVA: gene set variation analysis for microarray and RNA-seq data. BMC Bioinformatics. 14:7. 10.1186/1471-2105-14-7
23. Subramanian A, Tamayo P, Mootha VK, Mukherjee S, Ebert BL, Gillette MA et al (2005) Gene set enrichment analysis: a knowledge-based approach for interpreting genome-wide expression profiles. Proc Natl Acad Sci U S A. 102(43):15545-15550. 10.1073/pnas.0506580102
24. Barbie DA, Tamayo P, Boehm JS, Kim SY, Moody SE, Dunn IF et al (2009) Systematic RNA interference reveals that oncogenic KRAS-driven cancers require TBK1. Nature. 462(7269):108-112. 10.1038/nature08460
25. Charoentong P, Finotello F, Angelova M, Mayer C, Efremova M, Rieder D et al (2017) Pan-cancer Immunogenomic Analyses Reveal Genotype-Immunophenotype Relationships and Predictors of

Response to Checkpoint Blockade. Cell Rep. 18(1):248-262. 10.1016/j.celrep.2016.12.019

26. Deng S, Zhang H, Zhu K, Li X, Ye Y, Li R et al (2021) M6A2Target: a comprehensive database for targets of m6A writers, erasers and readers. Brief Bioinform. 22(3). 10.1093/bib/bbaa055
27. Ritchie ME, Phipson B, Wu D, Hu Y, Law CW, Shi W et al (2015) limma powers differential expression analyses for RNA-sequencing and microarray studies. Nucleic Acids Res. 43(7):e47. 10.1093/nar/gkv007
28. Batlle E, Massague J (2019) Transforming Growth Factor-beta Signaling in Immunity and Cancer. Immunity. 50(4):924-940. 10.1016/j.immuni.2019.03.024
29. Meurette O, Mehlen P (2018) Notch Signaling in the Tumor Microenvironment. Cancer Cell. 34(4):536-548. 10.1016/j.ccell.2018.07.009
30. Doheny D, Manore SG, Wong GL, Lo HW (2020) Hedgehog Signaling and Truncated GLI1 in Cancer. Cells. 9(9). 10.3390/cells9092114
31. Katoh M, Katoh M (2020) Precision medicine for human cancers with Notch signaling dysregulation (Review). Int J Mol Med. 45(2):279-297. 10.3892/ijmm.2019.4418
32. Jiang Y, Wang C, Zhou S (2020) Targeting tumor microenvironment in ovarian cancer: Premise and promise. Biochim Biophys Acta Rev Cancer. 1873(2):188361. 10.1016/j.bbcan.2020.188361
33. Cheng M, Sheng L, Gao Q, Xiong Q, Zhang H, Wu M et al (2019) The m(6)A methyltransferase METTL3 promotes bladder cancer progression via AFF4/NF-kappaB/MYC signaling network. Oncogene. 38(19):3667-3680. 10.1038/s41388-019-0683-z
34. Hua W, Zhao Y, Jin X, Yu D, He J, Xie D et al (2018) METTL3 promotes ovarian carcinoma growth and invasion through the regulation of AXL translation and epithelial to mesenchymal transition. Gynecol Oncol. 151(2):356-365. 10.1016/j.ygyno.2018.09.015
35. Liu T, Wei Q, Jin J, Luo Q, Liu Y, Yang Y et al (2020) The m6A reader YTHDF1 promotes ovarian cancer progression via augmenting EIF3C translation. Nucleic Acids Res. 48(7):3816-3831. 10.1093/nar/gkaa048
36. Liu J, Eckert MA, Harada BT, Liu SM, Lu Z, Yu K et al (2018) m(6)A mRNA methylation regulates AKT activity to promote the proliferation and tumorigenicity of endometrial cancer. Nat Cell Biol. 20(9):1074-1083. 10.1038/s41556-018-0174-4
37. Cong P, Wu T, Huang X, Liang H, Gao X, Tian L et al (2021) Identification of the Role and Clinical Prognostic Value of Target Genes of m6A RNA Methylation Regulators in Glioma. Front Cell Dev Biol. 9:709022. 10.3389/fcell.2021.709022
38. Song W, Ren J, Yuan W, Xiang R, Ge Y, Fu T (2021) N6-Methyladenosine-Related lncRNA Signature Predicts the Overall Survival of Colorectal Cancer Patients. Genes (Basel). 12(9). 10.3390/genes12091375
39. Liu Z, Zhong J, Zeng J, Duan X, Lu J, Sun X et al (2021) Characterization of the m6A-Associated Tumor Immune Microenvironment in Prostate Cancer to Aid Immunotherapy. Front Immunol. 12:735170. 10.3389/fimmu.2021.735170

40. Yang X, Wu W, Pan Y, Zhou Q, Xu J, Han S (2020) Immune-related genes in tumor-specific CD4(+) and CD8(+) T cells in colon cancer. BMC Cancer. 20(1):585. 10.1186/s12885-020-07075-x
41. Dazhi W, Zheng J, Chunling R (2020) High ELK3 expression is associated with the VEGF-C/VEGFR-3 axis and gastric tumorigenesis and enhances infiltration of M2 macrophages. Future Med Chem. 12(24):2209-2224. 10.4155/fmc-2019-0337
42. Meng L, Xing Z, Guo Z, Liu Z (2020) LINC01106 post-transcriptionally regulates ELK3 and HOXD8 to promote bladder cancer progression. Cell Death Dis. 11(12):1063. 10.1038/s41419-020-03236-9
43. Kim HK, Park JD, Choi SH, Shin DJ, Hwang S, Jung HY et al (2020) Functional Link between miR-200a and ELK3 Regulates the Metastatic Nature of Breast Cancer. Cancers (Basel). 12(5). 10.3390/cancers12051225
44. Wu F, Nie S, Yao Y, Huo T, Li X, Wu X et al (2021) Small-molecule inhibitor of AF9/ENL-DOT1L/AF4/AFF4 interactions suppresses malignant gene expression and tumor growth. Theranostics. 11(17):8172-8184. 10.7150/thno.56737
45. Liang K, Smith ER, Aoi Y, Stoltz KL, Katagi H, Woodfin AR et al (2018) Targeting Processive Transcription Elongation via SEC Disruption for MYC-Induced Cancer Therapy. Cell. 175(3):766-779 e717. 10.1016/j.cell.2018.09.027
46. Han J, Wang JZ, Yang X, Yu H, Zhou R, Lu HC et al (2019) METTL3 promote tumor proliferation of bladder cancer by accelerating pri-miR221/222 maturation in m6A-dependent manner. Mol Cancer. 18(1):110. 10.1186/s12943-019-1036-9
47. Routh ED, Pullikuth AK, Jin G, Chifman J, Chou JW, D'Agostino RB, Jr. et al (2020) Transcriptomic Features of T Cell-Barren Tumors Are Conserved Across Diverse Tumor Types. Front Immunol. 11:57. 10.3389/fimmu.2020.00057
48. Park DE, Cheng J, McGrath JP, Lim MY, Cushman C, Swanson SK et al (2020) Merkel cell polyomavirus activates LSD1-mediated blockade of non-canonical BAF to regulate transformation and tumorigenesis. Nat Cell Biol. 22(5):603-615. 10.1038/s41556-020-0503-2
49. Xiong Y, Wang L, Di Giorgio E, Akimova T, Beier UH, Han R et al (2020) Inhibiting the coregulator CoREST impairs Foxp3+ Treg function and promotes antitumor immunity. J Clin Invest. 130(4):1830-1842. 10.1172/JCI131375
50. Musolf AM, Simpson CL, Moiz BA, Pikielny CW, Middlebrooks CD, Mandal D et al (2021) Genetic Variation and Recurrent Haplotypes on Chromosome 6q23-25 Risk Locus in Familial Lung Cancer. Cancer Res. 81(12):3162-3173. 10.1158/0008-5472.CAN-20-3196
51. Wang LE, Gorlova OY, Ying J, Qiao Y, Weng SF, Lee AT et al (2013) Genome-wide association study reveals novel genetic determinants of DNA repair capacity in lung cancer. Cancer Res. 73(1):256-264. 10.1158/0008-5472.CAN-12-1915
52. Chen X, Wang P, Wang S, Li J, Ou T, Zeng X (2019) CIZ1 knockdown suppresses the proliferation of bladder cancer cells by inducing apoptosis. Gene. 719:143946. 10.1016/j.gene.2019.143946
53. Pauzaite T, Thacker U, Tollitt J, Copeland NA (2016) Emerging Roles for Ciz1 in Cell Cycle Regulation and as a Driver of Tumorigenesis. Biomolecules. 7(1). 10.3390/biom7010001

54. Higgins G, Roper KM, Watson IJ, Blackhall FH, Rom WN, Pass HI et al (2012) Variant Ciz1 is a circulating biomarker for early-stage lung cancer. Proc Natl Acad Sci U S A. 109(45):E3128-3135. 10.1073/pnas.1210107109
55. Monteverde T, Tait-Mulder J, Hedley A, Knight JR, Sansom OJ, Murphy DJ (2018) Calcium signalling links MYC to NUAK1. Oncogene. 37(8):982-992. 10.1038/onc.2017.394
56. Phippen NT, Bateman NW, Wang G, Conrads KA, Ao W, Teng PN et al (2016) NUAK1 (ARK5) Is Associated with Poor Prognosis in Ovarian Cancer. Front Oncol. 6:213. 10.3389/fonc.2016.00213
57. Zhang HY, Li JH, Li G, Wang SR (2015) Activation of ARK5/miR-1181/HOXA10 axis promotes epithelial-mesenchymal transition in ovarian cancer. Oncol Rep. 34(3):1193-1202. 10.3892/or.2015.4113
58. Riester M, Wei W, Waldron L, Culhane AC, Trippa L, Oliva E et al (2014) Risk prediction for late-stage ovarian cancer by meta-analysis of 1525 patient samples. J Natl Cancer Inst. 106(5). 10.1093/jnci/dju048
59. Kinzler KW, Nilbert MC, Vogelstein B, Bryan TM, Levy DB, Smith KJ et al (1991) Identification of a gene located at chromosome 5q21 that is mutated in colorectal cancers. Science. 251(4999):1366-1370. 10.1126/science.1848370
60. Fukuyama R, Niculaita R, Ng KP, Obusez E, Sanchez J, Kalady M et al (2008) Mutated in colorectal cancer, a putative tumor suppressor for serrated colorectal cancer, selectively represses beta-catenin-dependent transcription. Oncogene. 27(46):6044-6055. 10.1038/onc.2008.204
61. Xiao J, Lv D, Zhou J, Bei Y, Chen T, Hu M et al (2017) Therapeutic Inhibition of miR-4260 Suppresses Colorectal Cancer via Targeting MCC and SMAD4. Theranostics. 7(7):1901-1913. 10.7150/thno.19168
62. Li W, Xu M, Li Y, Huang Z, Zhou J, Zhao Q et al (2020) Comprehensive analysis of the association between tumor glycolysis and immune/inflammation function in breast cancer. J Transl Med. 18(1):92. 10.1186/s12967-020-02267-2
63. Lazear HM, Schoggins JW, Diamond MS (2019) Shared and Distinct Functions of Type I and Type III Interferons. Immunity. 50(4):907-923. 10.1016/j.immuni.2019.03.025

Figures

Figure 1

The flow chart of the study conducted.

Figure 2

Survival analysis of m6A regulators in TCGA datasets and GSE140082. High expression of *CBLL1* (A), *FTO* (B), *HNRNPC* (C), *METTL3* (D), *METTL14* (E), *WTAP* (G), and *ZC3H13* (I) and low expression of *RBM15B* (F) and *YTHDC2* (H) were associated with worse OS. Note: OS, overall survival.

Figure 3

Clinical and biological characteristics of three m6A modification patterns. (A) The interaction between m6A regulators in ovarian cancer. The circle size represented the effect of each regulator on the prognosis. The right semicircle represents whether a gene is a risk factor or a favorable factor. Purple dots in the right semicircle, risk factors of prognosis; Green dots in the right semicircle, protective factors of prognosis. On the other hand, the left semicircle color represents the type of m6A. Red dots in the left semicircle, erasers of m6A regulators; Orange dots in the left semicircle, readers of m6A regulators; Grey dots in the left semicircle, writers off m6A regulators. The lines linking regulators showed their interactions. Negative correlation was marked with blue and positive correlation with pink. (B) Survival analysis for the three m6A modification patterns based on 756 patients with ovarian cancer from TCGA cohorts (376 cases) and GSE140082 (380 cases). (C) The heatmap of clinicopathologic characters in three clusters (cluster A/B/C).

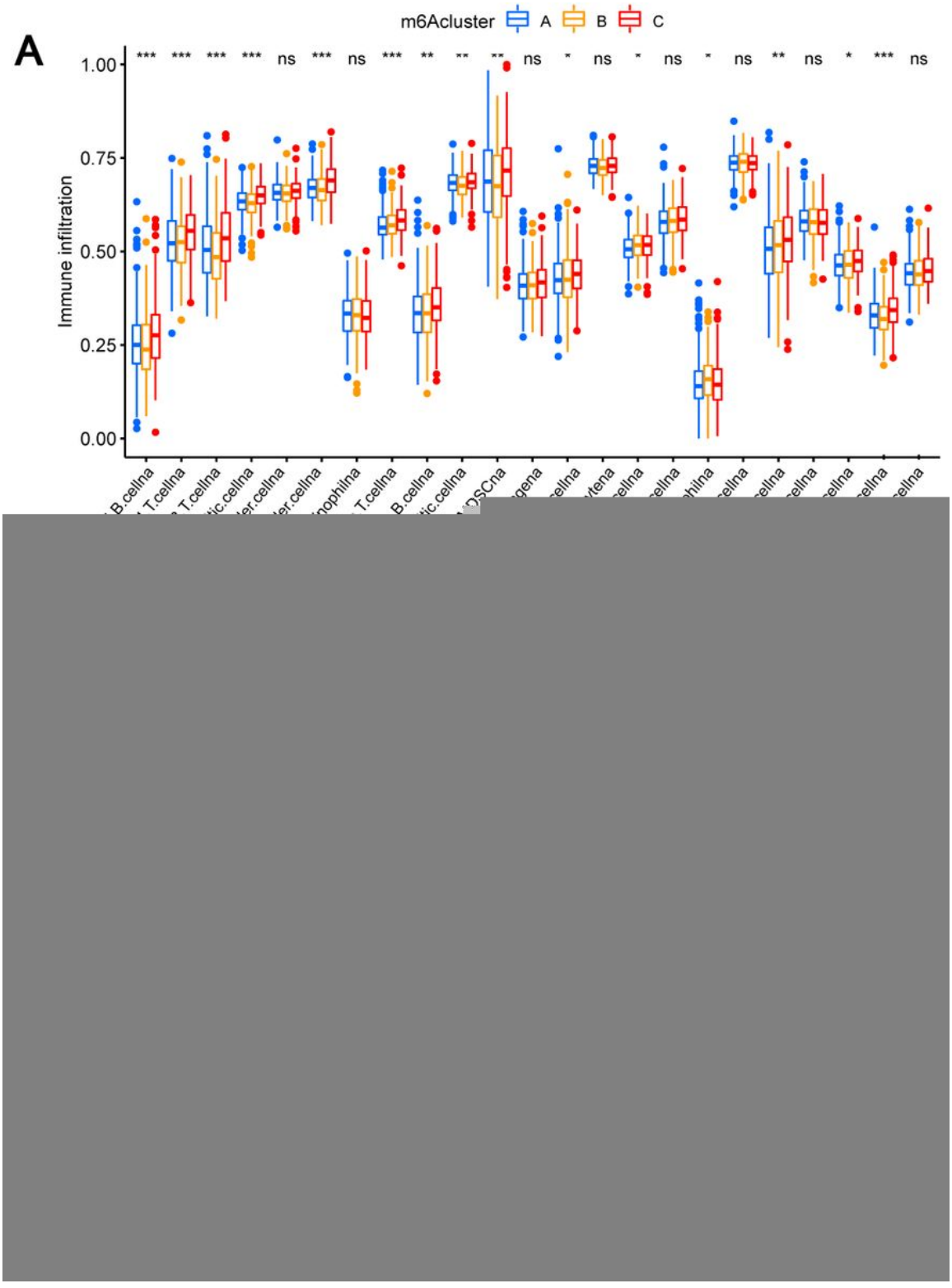

Figure 4

Immune landscape of three patterns. (A) The correlation between 9 prognostic m6A and TME infiltration cell type. Red color means positive correlated and blue color means negative correlated. (B) Immune infiltration analysis in three clusters. Cluster A, blue; cluster B, orange; cluster C, red.

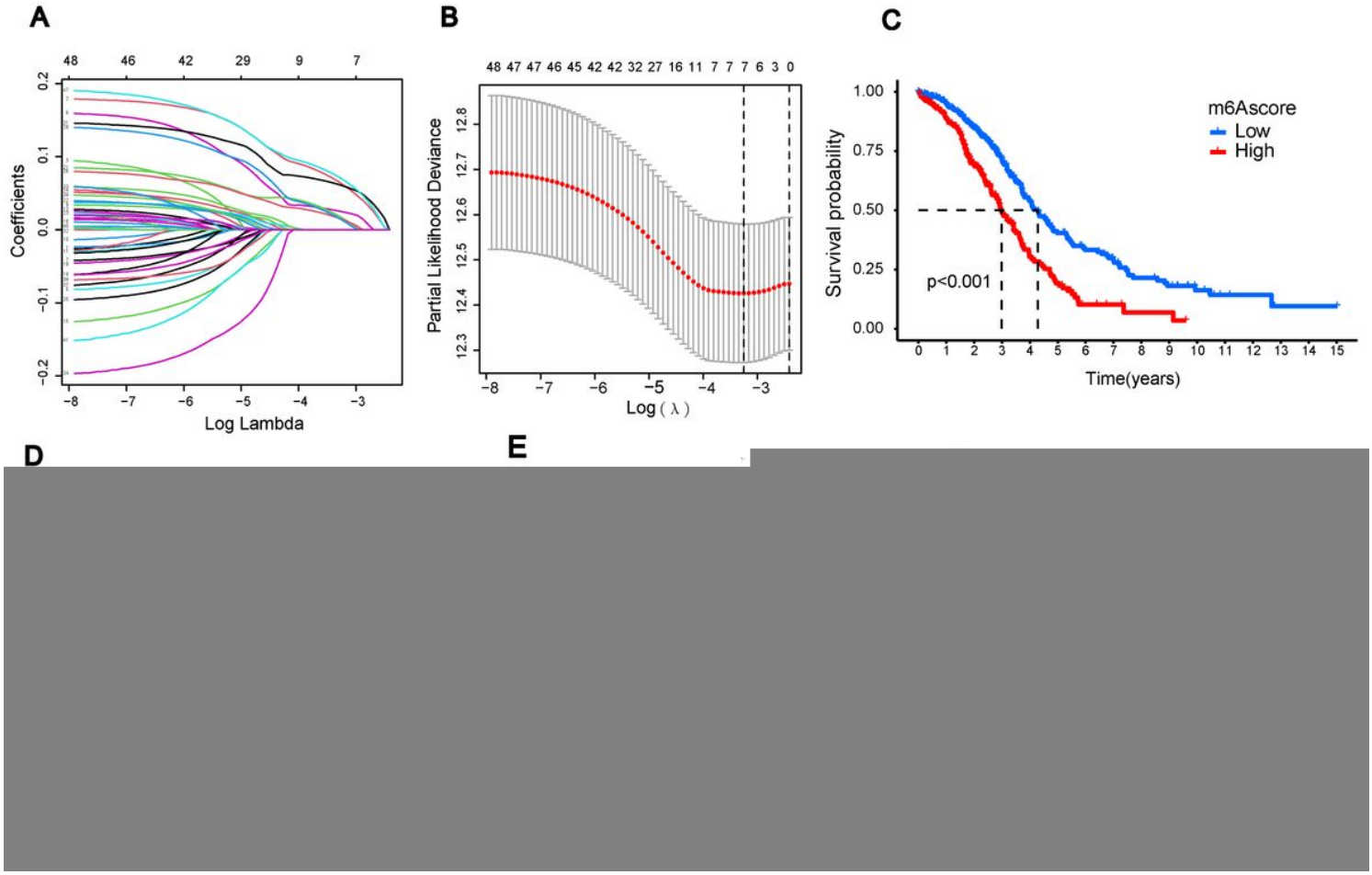

Figure 5

Construction of m6A score model. (A) The coefficient of interferon gamma response genes was calculated and seven genes (B) were screened by LASSO regression analysis. (C) Survival analyses for patients in high- and low- risk group using Kaplan-Meier curves ($p < 0.001$, log-rank test). (D) Five years' AUC of time-independent ROC curves. (E) T-SNE and PCA (F) analysis of ovarian cancer patients.

Figure 6

The immune landscape in risk groups. (A) Differences of stromal score, immune score and estimate score between risk high-score and low-score. (B) The abundance of TME infiltrating cell. The expression of 13 immune-related functions (C), cell proliferation related gene (D), DNA repair related gene (E), HLA related gene (F) and EMT related gene (G) between two risk groups.

Figure 7

Evaluation of the potential efficacy of immunotherapy in two risk groups. The expression of immune checkpoint (A) and IPS (B) between two groups. (C) Spearman analysis of m6Ascore and TMB. (D) Survival analysis of low and high TMB patients in TCGA cohort. (E) Survival analysis of subgroup patients stratified by risk score and TMB. (F) The expression of TMB in high- and low-risk groups. The waterfall plot of tumor somatic mutation established in high- (G) and low-risk group (H).

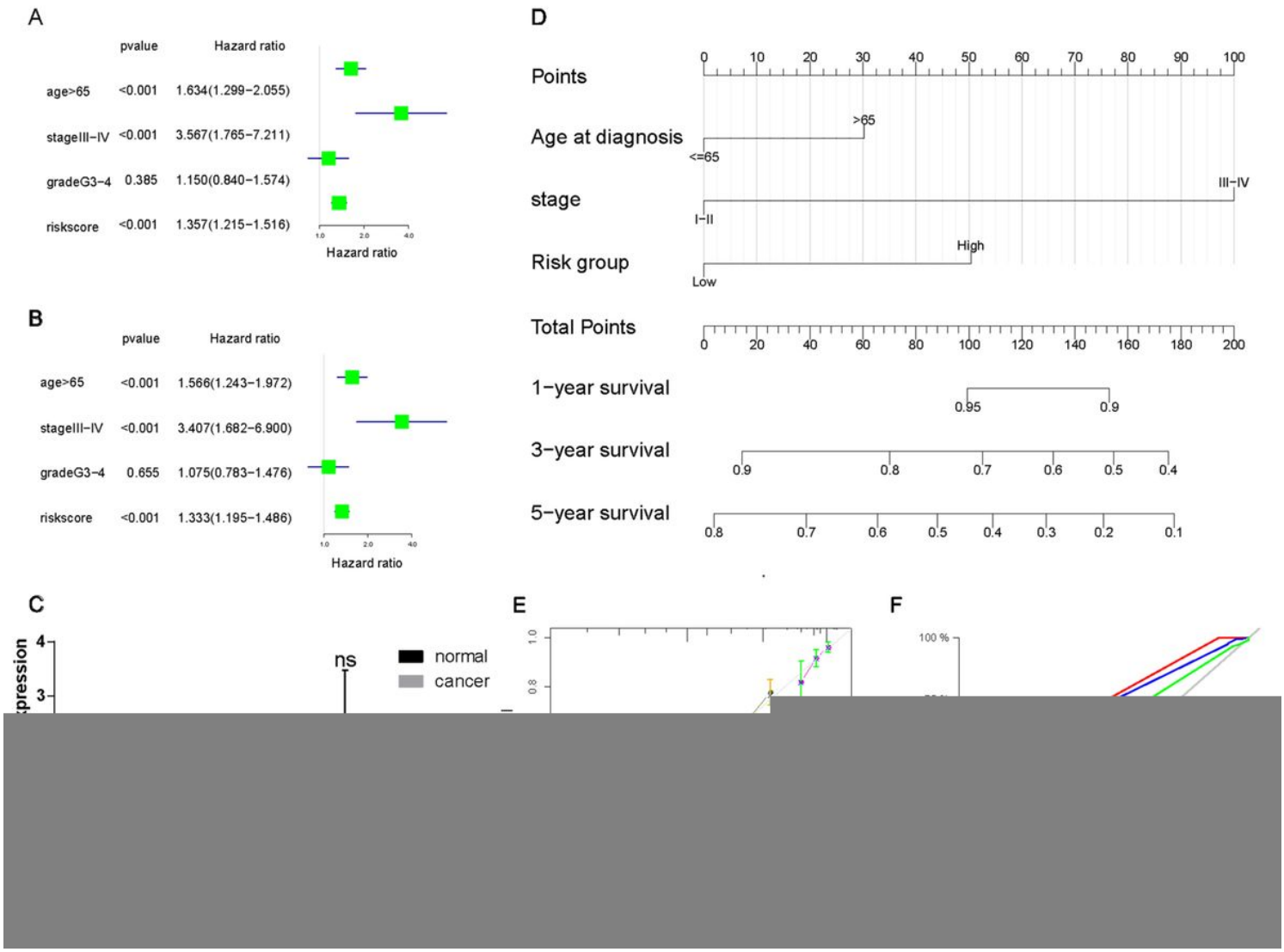

Figure 8

Validation and application of risk score in ovarian cancer. (A-B) Univariate analysis (A) and multivariate analysis (B) of the hazard ratios for risk score. (C) The expression of seven genes in normal ovary tissue (n=3) and ovarian cancer tissue (n=5) by qRT-PCR. (D) A nomogram to quantitatively predict survival based on risk score and clinical parameters. Calibration curves (E) of the nomogram and receiver operating characteristic (ROC) curves (F) to estimate the accuracy and performance of the predictive nomogram.

Supplementary Files

This is a list of supplementary files associated with this preprint. Click to download.

- ESM1.pdf
- ESM2.pdf
- ESM3.pdf
- ESM4.pdf
- ESM5.pdf
- ESM6.pdf
- ESM7.pdf
- ESM8.xls